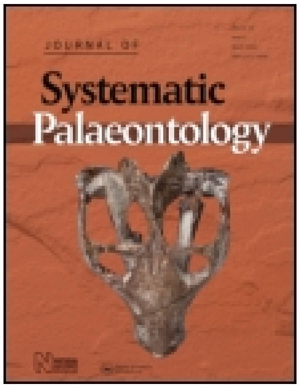

Journal of Systematic Palaeontology
Publication details, including instructions for authors and subscription information:
http://www.tandfonline.com/loi/tjsp20

An almost complete skeleton of a new Mesotheriidae (Notoungulata) from the Late Miocene of Casira, Bolivia

Esperanza Cerdeño [a], Bárbara Vera [a], Gabriela Inés Schmidt [b], François Pujos [a c] & Bernardino Mamaní Quispe [d]

[a] Departamento de Paleontología, IANIGLA, CCT-CONICET-Mendoza. Avda. Ruiz Leal s/n, 5500, Mendoza, Argentina

[b] Laboratorio de Paleontología de Vertebrados, CICYTTP-CONICET, Matteri y España, 3105, Diamante, Argentina

[c] Instituto Francés de Estudios Andinos, Av. Arequipa 4595, Lima 18, Peru

[d] Departamento de Paleontología, Museo Nacional de Historia Natural, La Paz. Calle 26 s/n, Cota Cota, La Paz, Bolivia

To cite this article: Esperanza Cerdeño, Bárbara Vera, Gabriela Inés Schmidt, François Pujos & Bernardino Mamaní Quispe (2012): An almost complete skeleton of a new Mesotheriidae (Notoungulata) from the Late Miocene of Casira, Bolivia, Journal of Systematic Palaeontology, 10:2, 341-360

To link to this article: http://dx.doi.org/10.1080/14772019.2011.569576

Journal of Systematic Palaeontology, Vol. 10, Issue 2, June 2012, 341–360

Taylor & Francis
Taylor & Francis Group

An almost complete skeleton of a new Mesotheriidae (Notoungulata) from the Late Miocene of Casira, Bolivia

Esperanza Cerdeño[a]*, Bárbara Vera[a], Gabriela Inés Schmidt[b], François Pujos[a,c] and Bernardino Mamaní Quispe[d]

[a]*Departamento de Paleontología, IANIGLA, CCT-CONICET-Mendoza. Avda. Ruiz Leal s/n, 5500 Mendoza, Argentina;* [b]*Laboratorio de Paleontología de Vertebrados, CICYTTP-CONICET, Matteri y España, 3105 Diamante, Argentina;* [c]*Instituto Francés de Estudios Andinos, Av. Arequipa 4595, Lima 18, Peru;* [d]*Departamento de Paleontología, Museo Nacional de Historia Natural, La Paz. Calle 26 s/n, Cota Cota, La Paz, Bolivia*

(Received 10 November 2010; accepted 11 December 2010; printed 16 May 2012)

A partial mesotheriine skeleton (Notoungulata, Mesotheriidae) from the Late Miocene Casira locality, southern Bolivia, is fully described and reinterpreted taxonomically. This specimen (MNHN-Bol-V-003724) was partially described previously without a taxonomic discussion, as it was considered to be *Plesiotypotherium* sp. After comparison with other Bolivian, Argentinean and Chilean mesotheres, we recognize a new species of the genus *Plesiotypotherium* Villarroel, *P. casirense* sp. nov., characterized by: nasals slightly enlarged posteriorly; zygomatic arch with strong antero-distal angle; zygomatic plate starting at the level of P4 and reaching the level of the anterior part of M3; lacrimal bony process; large infraorbital foramen; posterior border of the mandible very convex; P4 without lingual groove and with narrow and projected parastyle; M3 with simple third lobe; larger and more robust skeleton than other *Plesiotypotherium* species. Most postcranial elements are described in detail for the first time for *Plesiotypotherium*. The incomplete skull GB-KKL 740 from the same locality is also referred to the new taxon. *P. casirense* is the sister group of *P. achirense* Villarroel in the phylogenetic analysis, but the genus *Plesiotypotherium* appears as paraphyletic. The revised partial skull GB-ACH 100 from Achiri, Bolivia, which was labelled as *Plesiotypotherium* sp., does not belong to this genus, and it appears phylogenetically closer to *Pseudotypotherium* and *Mesotherium*. *Plesiotypotherium casirense* sp. nov. increases the known diversity of the Mesotheriidae in both the Miocene of Bolivia and the South American faunal context.

Keywords: Mesotheriinae; systematics; Neogene; Bolivia; South America

Introduction

The research cooperation between the Museo Nacional de Historia Natural (MNHN, La Paz, Bolivia) and the Instituto de Nivología, Glaciología y Ciencias Ambientales (IANIGLA, CCT-CONICET-Mendoza, Argentina) was recently consolidated in a MNHN-CONICET Agreement that allows and promotes palaeontological research in some areas of Bolivia (mainly in La Paz Department) and the study of former collections stored at the MNHN. In this context, we studied an almost complete skeleton of a Mesotheriidae (Notoungulata) from the locality of Casira (southern Bolivia).

Mesotheriinae mesotheriids are medium to large-sized notoungulates with rodentiform skull, and developed comparable habits to the present capybara. Their teeth are ever growing and the adult dental formula is 1/2, 0/0, 2/1, 3/3, with typical trilobed upper molars. The confused systematics of mesotheriids, mainly known from Argentina, was partially revised by Francis (1965) at the generic level, and those of Late Miocene age were later studied by Cerdeño and Montalvo (2001). In recent years, new studies are enlarging the knowledge of this group in different South American areas.

The specimen evaluated in this paper (MNHN-Bol-V-003724) was partially studied by Shockey *et al.* (2007) in their functional anatomical analysis of mesotheriids, but it was not described in detail nor taxonomically discussed. These authors considered it as *Plesiotypotherium* sp., although the collection label indicates cf. *Plesiotypotherium majus* Villarroel, 1974a. Together with this specimen, other mesotheriid remains were also revised, such as GB-ACH 228, an unpublished partial skull from the Mauri Formation of Achiri (Late Miocene, Bolivia; St-André, 1994) labelled *P. achirense* Villarroel, 1974a. Another specimen, GB-ACH 100, from Achiri is also labelled *Plesiotypotherium* sp., but its dental characteristics do not correspond to this genus (see below).

Few data have been previously published on the Casira (or Kasira) area. Anaya *et al.* (1989) reported a mesotheriid specimen (GB-KKL 740) recovered from the Casira Formation, outcropping in the Modesto Omiste Province,

---

*Corresponding author. Email: espe@mendoza-conicet.gob.ar

ISSN 1477-2019 print / 1478-0941 online

http://dx.doi.org/10.1080/14772019.2011.569576
http://www.tandfonline.com

Department of Potosí, near the border with Argentina. They described an incomplete skull and established the existence of cranial differences with respect to *Plesiotypotherium achirense*, but did not determine its taxonomic status.

Some Bolivian localities have yielded important Mesotheriidae specimens of different age, which have been recognized as distinct taxa (Villarroel 1974a, 1974b, 1978; Oiso 1991; Townsend & Croft 2010). Apart from the preliminary data on the mesothere from Casira (Anaya *et al.* 1989; Croft 2007; Shockey *et al.* 2007), no other studies have been carried out, despite the preservation of this almost complete skeleton. The aim of this paper is to provide both a detailed description of this very complete specimen and a thorough comparison with other Bolivian, Argentinean and Chilean mesotheres, in order to precisely describe its taxonomic and phylogenetic affinities.

Geographic and geological context

Following Anaya *et al.* (1989), the Casira Formation outcrops along the mountains located in the area of the eponymous locality, west of Chagua. It is constituted of basal conglomerates, whitish to yellow-greyish (sometimes greenish) friable tuffs, and interbedding sandy, sand-clayish sediments, light-coloured clays, and conglomerates. At the top of the sequence, there are grey agglomerates, microagglomerate horizons, tuffs, and clays. The age of the Casira Formation was never well established (Anaya *et al.* 1989; Croft 2007).

There are no precise data on the stratigraphic origin (geographical coordinates are not known) of the studied skeleton with respect to the skull previously described by Anaya *et al.* (1989), but they probably come from the same levels of the Casira Formation. This is based on the fact that the label accompanying specimen MNHN-Bol-V-003724 ("Provincia Modesto Omiste- Depto. Potosí, 55 km NW Villazón"; Fig. 1) refers to the same area published for the skull GB-KKL 740, and that the latter was studied by the same researcher (F. Anaya) who years later collected the skeleton MNHN-Bol-V 003724.

Institutional abbreviations

GB: Servicio Geológico de Bolivia (palaeontological collection presently stored at the MNHN-Bol); **GHUNL-Pam**: Departamento de Geología Histórica, Facultad de Ciencias Exactas y Naturales, Universidad Nacional de La Pampa; **MLP**: Museo de La Plata; **MNHN-Bol**: Museo Nacional de Historia Natural-Bolivia.

Anatomical and dimensional abbreviations

APD, anteroposterior diameter; **ant.**, anterior; **art.**, articulation; **dis.**, distal; **epi.**, epiphysis; **H**, height; **I/i**, upper/lower incisors; **L**, length; **M/m**, upper/lower molars; **Mc/Mt**, metacarpal/metatarsal; **P/p**, upper/lower premolars; **prox.**, proximal; **TD**, transversal diameter.

Figure 1. Location of the Casira area, Bolivia.

Materials and methods

The studied material was collected by Federico Anaya and Pierre-Antoine Saint-André, and in 1996 was stored in the vertebrate palaeontological collection of the MNHN, La Paz (Bolivia), under the reference number MNHN-Bol-V 003724. The skeleton is composed of the greater part of a single individual very well preserved, with only the scapula, femur, pyramidal, entocuneiform and cuboid missing. Measurements were taken with a caliper and expressed in millimetres.

For descriptions, we considered six main faces of each element: proximal (or dorsal in the skull), distal (or ventral in the skull), anterior, posterior (occipital in the skull), medial and lateral; we considered the anterior to be the head position, medial to be the sagittal plane, and lateral to be the external side of the body. Limb bones are considered in a unique vertical axis independently of the actual anatomical position.

To evaluate the phylogenetic affinities of MNHN-Bol-V 003724, we performed a cladistic analysis of mesotheriines based on previous analyses by Cerdeño & Montalvo (2001), Croft *et al.* (2004) and Flynn *et al.* (2005). Details are presented in the Phylogenetic Analysis section.

Systematic descriptions

Order **Notoungulata** Roth, 1903
Family **Mesotheriidae** Alston, 1876
Genus ***Plesiotypotherium*** Villarroel, 1974a

Comment. *Plesiotypotherium* is not well supported phylogenetically (see Phylogenetic Analysis for further comments on diagnostic characters established by Villarroel, 1974a).

Plesiotypotherium casirense sp. nov.
(Figs 2–7)

2007 *Plesiotypotherium* sp.; Shockey *et al.*: 227–247.

Diagnosis. Species of *Plesiotypotherium* differing from *P. achirense* and *P. majus* by zygomatic arch with strong anterodistal angle (autapomorphy); zygomatic plate with concave posterior border, reaching the level of the anterior part of M3 (autapomorphy); zygomatic arch starting at the level of P4; nasals proportionally less enlarged posteriorly, with the posterior border not so markedly W-shaped; wider mandibular incision between the coronoid process and the mandibular condyle; posterior border of the mandible clearly more convex; P4 with narrower and more projected parastyle, with more marked groove, and more convex paracone fold; M3 with simple third lobe; larger size and more robust postcranial skeleton. Parallel or gently convex diastema is a synapomorphic character shared with *Typotheriopsis*, *Caraguatypotherium* and *Pseudotypotherium*. The presence of a lacrimal bony process is a synapomorphy of *P. casirense* and *P. achirense*. The large infraorbital foramen is shared with *Plesiotypotherium achirense* and two species of *Pseudotypotherium*, *Ps. subinsigne and Ps. exiguum*. The absence of lingual groove in P4 and the triangular-outlined upper premolars are features shared with *Typotheriopsis* and different from *Caraguatypotherium*, *Pseudotypotherium* or *Mesotherium*.

Derivation of name. From Casira, the type locality.

Holotype. MNHN-Bol-V 003724, rather complete skeleton from Casira, Bolivia.

Referred material. GB-KKL 740, incomplete skull from Casira, Bolivia.

Table 1. Skull and mandible dimensions (mm) of the specimen MNHN-Bol-V 003724 of *Plesiotypotherium casirense* sp. nov.

Skull	
Total length	(248)
Nasal length	111.7
Anterior nasal width	41.1
Posterior nasal width	65.26
Maxillary width	66.9
Maximum frontal width (estimate)	(120)
Maximum zygomatic width (estimate)	(168)
Zygomatic maximum length	107.0
Zygomatic anterior length	17.3
Zygomatic maximum height	64.9
Zygomatic minimum height	26.5
Orbit	(26) × 36.5
Maximal width at occipital condyles	54.7
Maximal width at paraoccipital apoph.	73.6
Maximal width at posttympanic apoph.	104.7
Ventral length of premaxillary	31.0
Ventral width of premaxillary	40.2
Maxillary height ahead P3 level	49.9
Palatal length	138.4
Palatal width	68.0
Length P3–M3	76.4
Mandible	
Maximum length (to the incisor alveololi)	214
Maximum height	133
H horizontal ramus at diastema	40.7
H horizontal ramus at p4–m1	42.2
H behind m3	59.5
H at mandibular incision	112.1
H at condyle	124.9
Maximum width at symphysis	35.2
Minimum width at borders of diastema	24.6

Occurrence. Casira locality, 55 km NW Villazón, Modesto Omiste Province, Potosí Department, Bolivia. Late Miocene levels of the Casira Formation.

Description

Skull (Fig. 2; Table 1). It lacks part of the occipital and frontal bones and the left zygomatic arch. Nasal bones are slightly convex anteriorly; they show little variation in width, and the anterior tip narrows slightly. The nasal opening is very shallow in lateral view. The maxilla overlaps the nasal bone all along its border. The nasal suture is not fused anteriorly. The posterior border is rounded, almost straight in the middle. The preserved right frontal bone presents a large postorbital apophysis that contacts with the zygomatic arch and closes the orbit. Dorsally, the frontal strongly narrows behind the postorbital apophyses, enlarging immediately backwards (Fig. 2B). The arch begins at the level of P4 (better observed ventrally than laterally), bends downwards forming a crest slightly directed posteriorly, and then forms a right angle with the inferior straight border, which is smoothly concave at its posterior end. It rises at an angle greater than 90°, forming a wide surface that is directed posteriorly and surpasses dorsally the postorbital apophysis

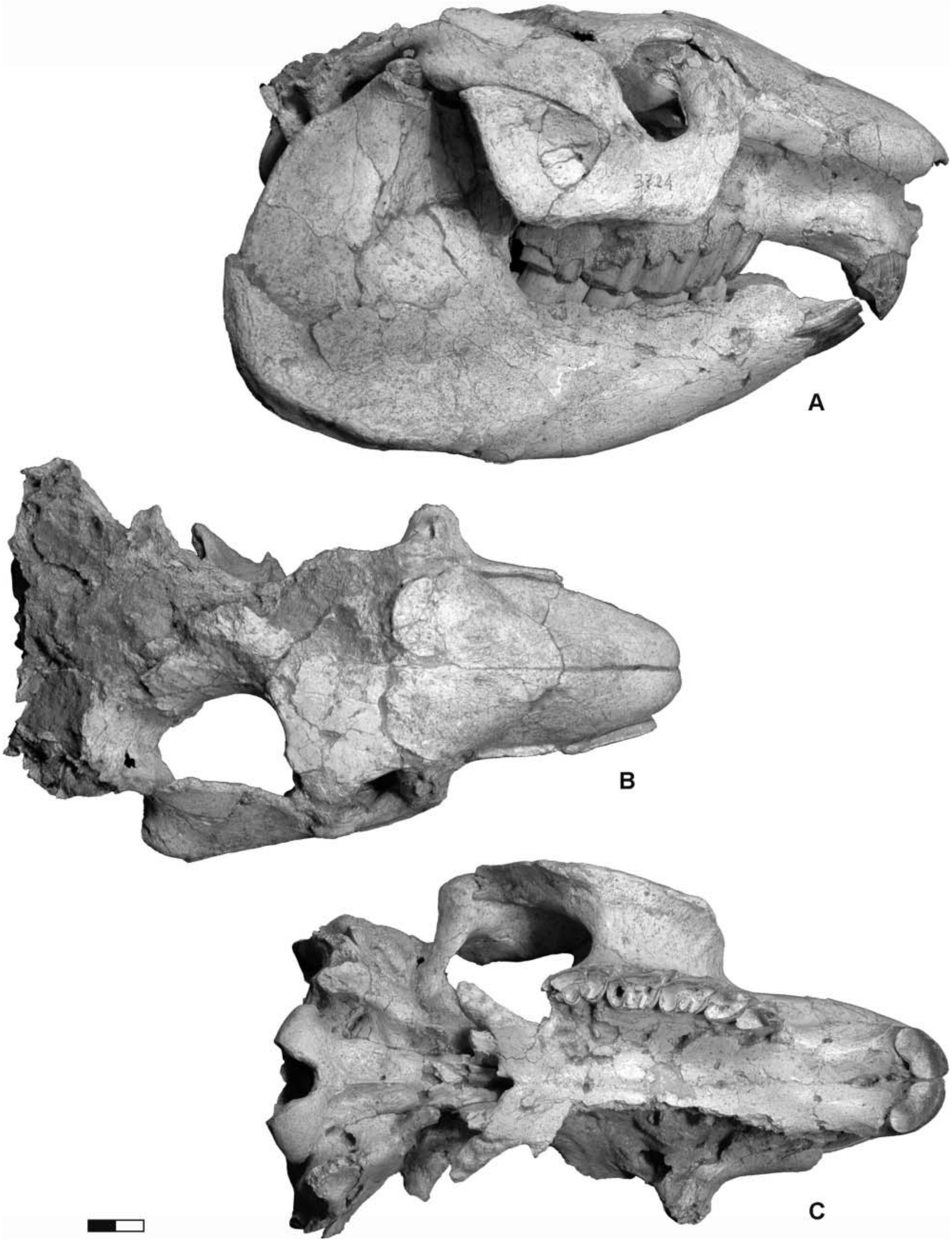

Figure 2. *Plesiotypotherium casirense* sp. nov. from Casira, MNHN-Bol-V 003724 **A,** skull and mandible, right lateral view; **B,** skull, dorsal view; **C,** skull, ventral view. Scale, 2 cm.

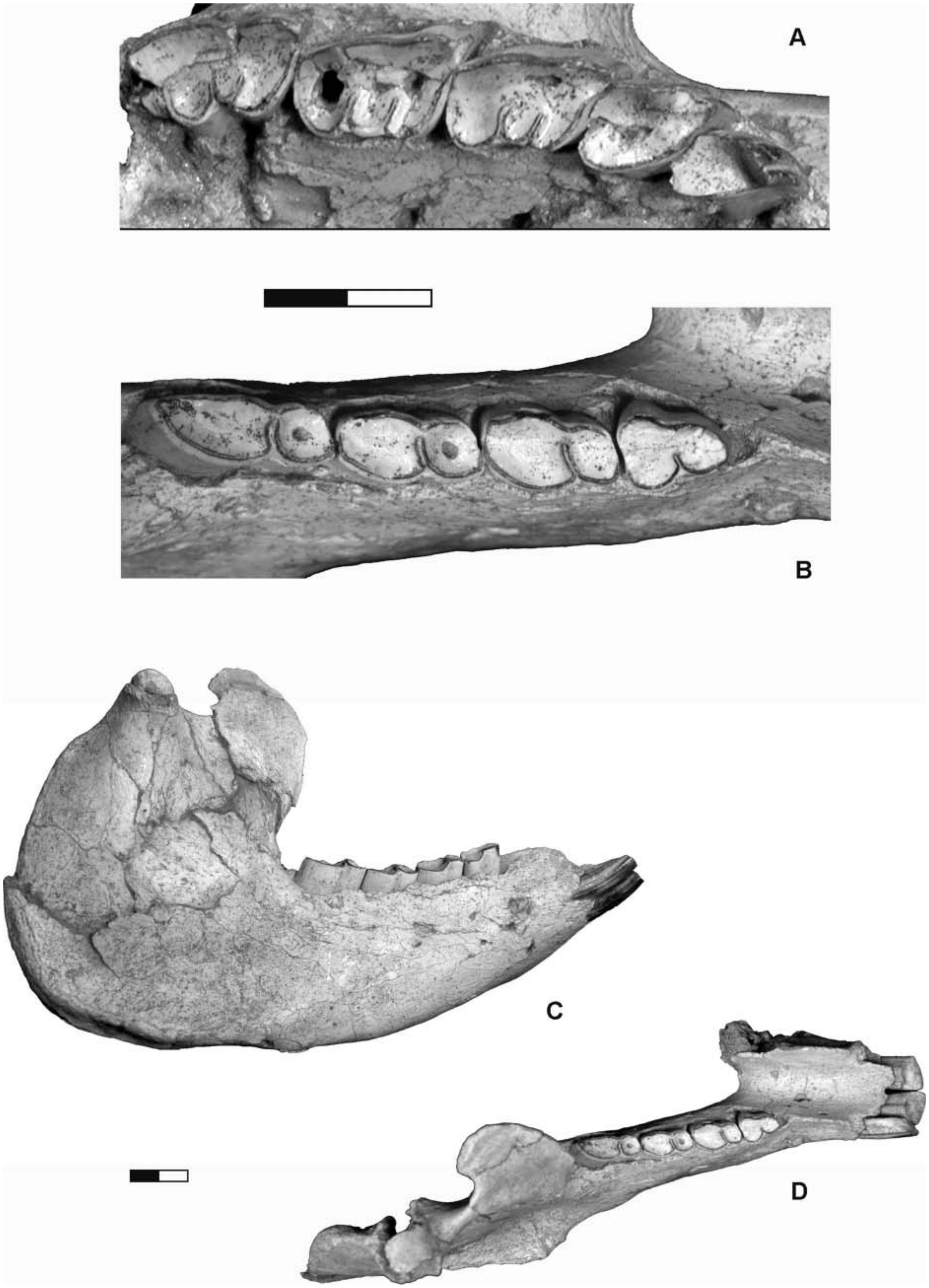

Figure 3. MNHN-Bol-V 003724 of *Plesiotypotherium casirense* sp. nov. from Casira: **A,** detail of the upper right series P3-M3; **B,** detail of the lower right series p4-m3; **C,** mandible, lateral view, **D,** mandible, occlusal view. Scales, 2 cm.

Figure 4. MNHN-Bol-V 003724 of *Plesiotypotherium casirense* sp. nov. from Casira: **A,** five dorsal vertebrae in anatomical connection; **B,** sacrum-right coxal, lateral view; **C,** right humerus, anterior and lateral views; **D,** left ulna, lateral and anterior views; **E,** left radius, posterior and anterior views. Scales, 2 cm.

(Fig. 2A). The posterodorsal border of the zygomatic arch is horizontal and bears the wide and short glenoid articulation. In the orbital portion, the arch develops a zygomatic plate, not very wide and somewhat inclined laterally; in the inner part, there is a small depression (the suborbital fossa as defined by Francis 1965) directed to the infraorbital foramen, which is large, rounded, and placed at the level of the anterior part of M1. The lacrimal bone is not very well preserved, but it presents one foramen together with a bony process that partially subdivides it.

Laterally, the premaxilla and maxilla form a depressed rostral face, where there are two small foramina (Fig. 2A). Laterally and posteriorly, the post-glenoid apophysis is short, narrow, and separated from the post-tympanic

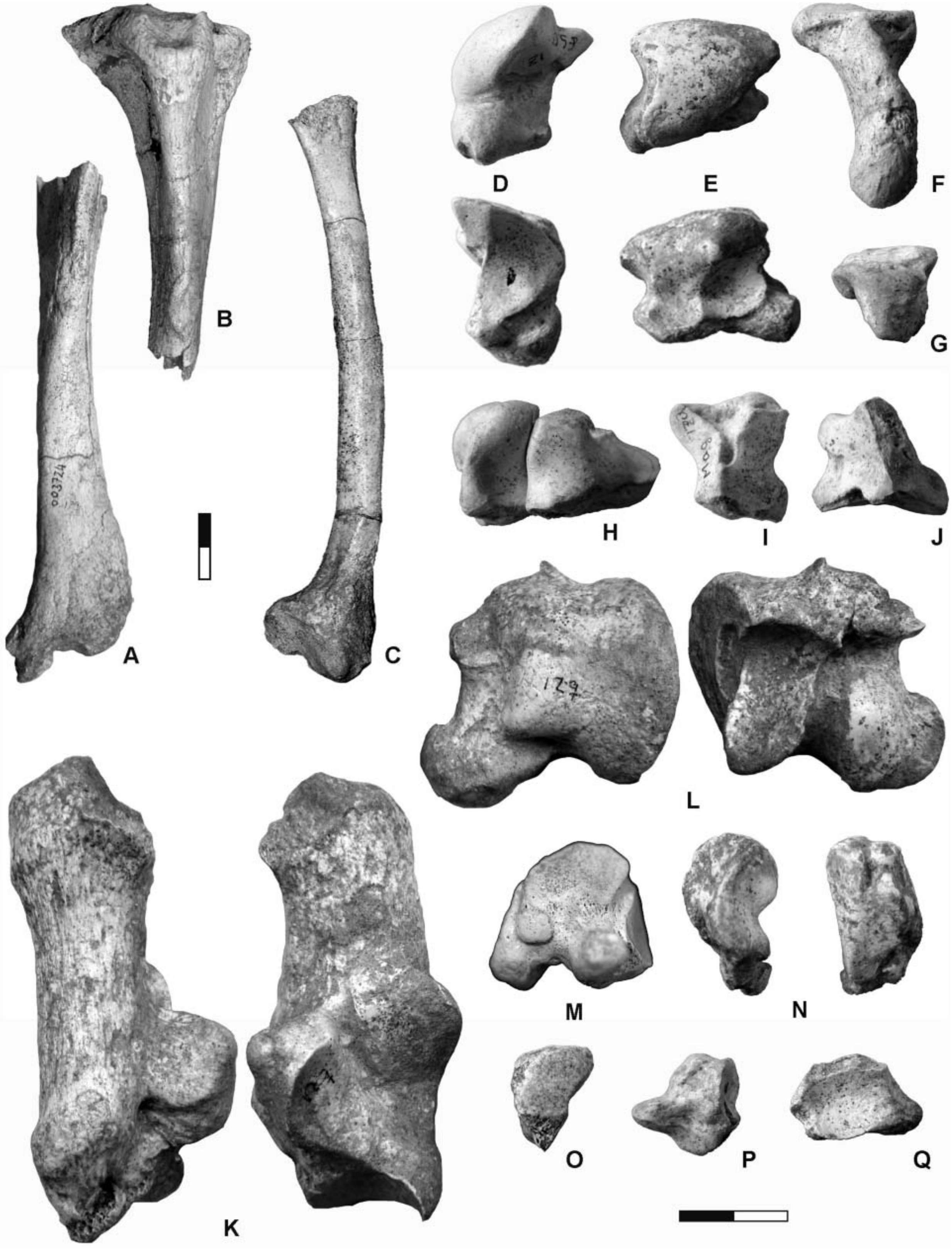

Figure 5. *Plesiotypotherium casirense* sp. nov. from Casira, MNHN-Bol-V 003724 **A,** left tibia without proximal end, anterior view; **B,** proximal half of right tibia, anterior view; **C,** left fibula, posteromedial view; **D,** right scaphoid, proximal and distal views; **E,** right semilunate, proximal and distal views, **F,** pisiform: proximal view; **G,** trapezoid, distal view; **H,** left magnum-unciform, proximal view; **I,** left magnum, distolateral view; **J,** left unciform, medial–anterior view; **K,** left calcaneum, posterior and anterolateral views; **L,** left astragalus, anterior and posterior views; **M,** left navicular, distal view; **N,** right mesocuneiform, proximal and distal views; **O,** left ectocuneiform, proximal view; **P,** left trapezium?, lateral view; **Q,** sesamoid, anterior view. Scales (A–C and D–Q), 2 cm.

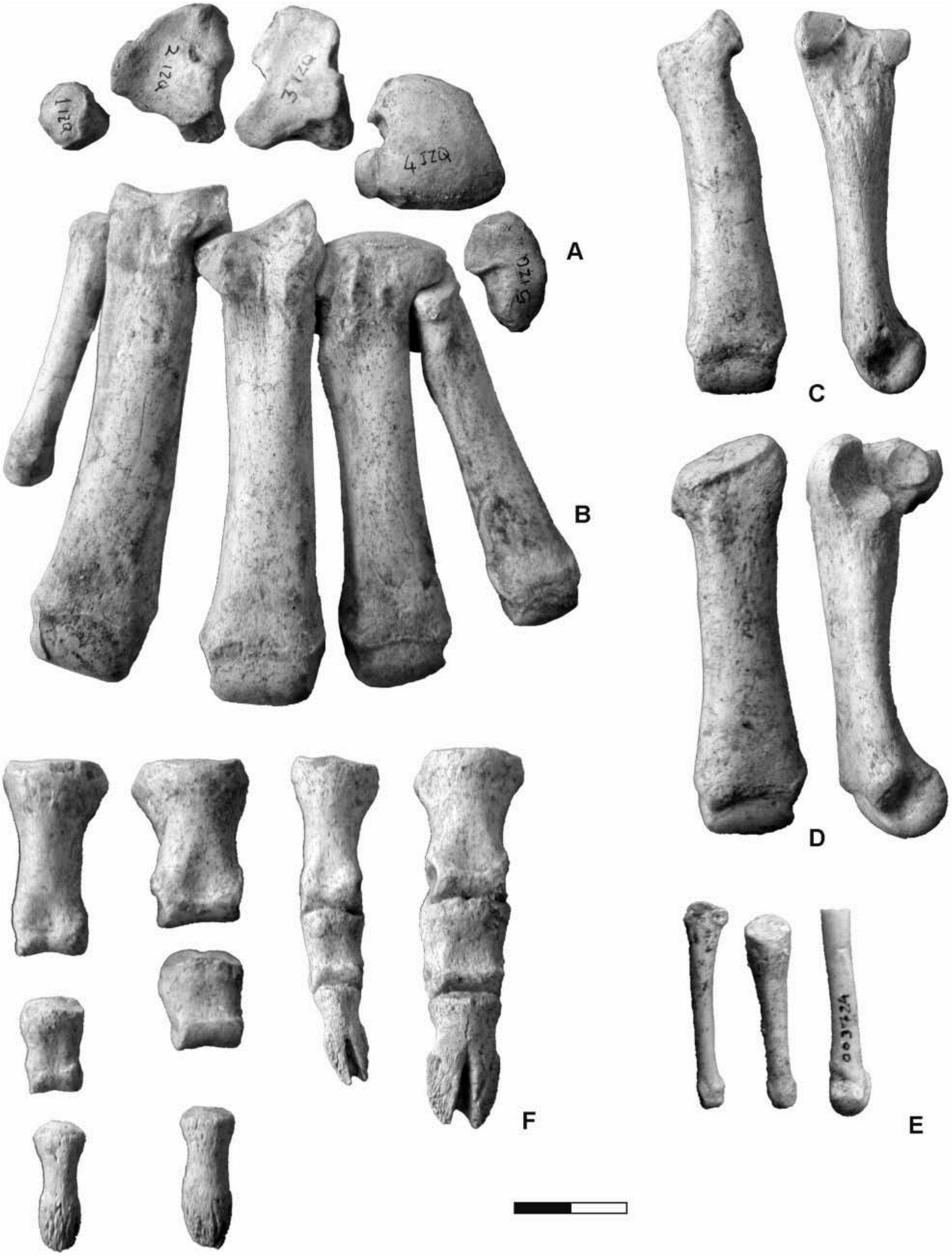

Figure 6. *Plesiotypotherium casirense* sp. nov. from Casira, MNHN-Bol-V 003724 **A,** McI to Mc V, proximal views; **B,** same bones, anterior view in anatomical position; **C,** left Mt II, anterior and lateral views; **D,** left Mt III, anterior and lateral views; **E,** reduced metapodials, probably Mt I or Mt V; **F,** first, second, and third phalanges showing proportional variations. Scale, 2 cm.

Figure 7. **A,** *Plesiotypotherium casirense* sp. nov. from Casira, skull GB-KKL 740 **B–D,** *P. achirense*, skull GB-ACH 228 **B,** dorsal view; **C,** ventral view; **D,** lateral view. Scales, 2 cm.

apophysis, which forms a longer plate, behind the auditory meatus, and is in contact with the paraoccipital apophysis. The latter is much more developed, long (lacking the apex) and transversely flattened.

The occipital condyles are small, each surrounded by one apophysis, leaving a small space between them. Ventrally, a foramen is observed at the base of each condyle, which could correspond to the hypoglossal foramen.

The palate is U-shaped at its anterior part, and enlarges posteriorly from the level of P3 (Fig. 2C). A long, smoothly concave diastema separates the incisor from the cheek-tooth series. The premaxillary–maxillary suture is placed at its posterior third and crosses the palate perpendicularly; two foramina are placed on the suture. The medial longitudinal suture presents a large post-incisor foramen, and two other small foramina are medially and posteriorly placed on it. The right major palatine foramen, badly preserved, opens at the P4-M1 level. The post-palatine apophyses and a great part of the palate are also preserved, as well as both I1 and the right series P3-M3. These apophyses are long and divergent, forming a wide angle. The post-palatal notch reaches the level of M3.

The whole basisphenoid is preserved. There are two narrow, pointed, forwardly directed apophyses that begin at the anterobasal portion of the post-tympanic and paraoccipital apophyses.

Mandible (Figs 2A, 3B–D; Table 1). It is incomplete, lacking the left horizontal and vertical rami, but symphysis is present with both pairs of incisors (left i2 broken inside the bone) and the right p4-m3 series is well preserved. The procumbent symphysis is relatively long and narrow, with high and acute proximal borders, slightly divergent backwards; it extends back to the level of the talonid of p4. The horizontal ramus presents a mental foramen below the posterior part of the diastema and other minor foramina more posteriorly placed (Fig. 3C). The inferior border of the ramus is convex, with a labial apophysis and an inflexion before the angular region. The latter is projected backwards and the posterior border is quite convex; the condyle is consequently much more anteriorly placed. The mandibular incision is short, and the coronoid apophysis is wide, slightly elevated, and medially curved.

Upper dentition (Figs 2C and 3A). The I1 are large, euhypsodont teeth (Table 2), obliquely implanted and kidney-outlined; the enamel is complete around the crown, finely and vertically striated, covered with cement; there is a

Table 2. Comparative dimensions (mm) of upper and lower dentition of *Plesiotypotherium casirense* sp. nov., MNHN-Bol-V 003724 *Holotype, Villarroel, 1974a; ***Plesiotypotherium* sp., Oiso (1991): minimum–maximum values, approximate eliminated. Minimum values for Nazareno lower teeth are rather small, maybe corresponding to juvenile individuals.

Bol-V-3724	I1	P3	P4	M1	M2	M3
L	20.7 21.9	9.9	12.5	18.2	18.9	21.2
Wa				11.5	13.4	12.3
Wm				11.3	11.7	10.4
Wp	12.0 13.2	9.6	11.7	11.2	11.2	11.8
P. achirense*						
L	(18.8)	9.6	10.7	17.0	18.7	19.8
W	(9.3)	8.5	10.0	11.0	12.2	10.8
GB AEH 228						
L	—	8.4 8.3	9.3 (9.4)	15.3 (15.6)	16.4 (15.6)	16.7 17.0
W	—	7.0 6.9	8.5 (8.7)	10.1 (10.7)	10.4 (12.0)	(10) (10)
P. majus*						
L	21.6	13.0	13.7	20.8	21.8	24.6
W	10.5	10.0	12.3	12.8	12.9	12.0
Nazareno**						
L	13.5–15.2	5.4–8.8	5.7–8.0	9.6–11.8	10.3–14.7	13.0–14.6
W	7.5–8.2	4.4–6.6	6.7–8.6	8.0–10.2	8.1–10.1	7.6–9.4
Bol-V-3724	i1	i2	p4	m1	m2	m3
L	12.4 12.9	7.0 6.3	12.6	16.8	17.7	21.3
Wa	7.8 8.1	7.8 5.9	6.4	8.0	8.5	8.3
Wp			9.6	10.2	9.2	8.3
P. achirense*						
L	11.0	7.5	11.8	15.0	16.0	22.5
W	6.7	5.2	8.2	9.7	9.2	8.5
Nazareno**						
L	7.5–9.2	4.7	8.4	7.7–10.8	8.5–11.4	8.1–18.1
W	5.3–6.2	3.3	6.1	5.2–8.0	4.8–8.5	3.9–7.2

marked lingual groove on the anterior third, and a second, hardly developed groove slightly backwards. Cheek teeth are relatively small (Table 2), with a cement layer all around the crown.

Premolars are triangular in outline, especially the P3, with a thin anterolabial groove. The labial face of P3 is convex, and the groove limits a thin parastyle; another groove, less marked, lies behind the paracone fold. The P4, well imbricated over P3, has a more flattened ectoloph and the anterolingual face more convex than P3; its paracone fold is more developed on the ectoloph. In labial view, the partially lacking bone allows the high crown of premolar to be seen.

The trilobed molars present a more undulose ectoloph. The parastyle projects forward, with little imbrication. Paracone and metacone folds are developed, the former more evident in M2. On the third lobe of M1 there is a short groove at the posterolingual angle, which is not present in M2-M3. The median lobe extends to the lingual face in M1-M2 whereas it is shorter in M3, although it is not lingually enclosed by the other two lobes.

Lower dentition (Fig. 3B, D). The first incisors are clearly larger than the i2 (Table 2). They have a smooth lingual groove, and present finely, vertically striated enamel; it is discontinuous, covering the labial face and a lingual band. There are traces of cement on the labial wall.

The p4 is subtriangular, with the anterior lobe much narrower than the posterior one (Table 2), but with similar length (around 6.5 mm); the labial groove is shallow and wide (as an open V in occlusal view); the lingual face is smoothly concave. First and second molars have the posterior lobe rounded, regularly convex labially and with smooth lingual grooves. The labial trigonid–talonid groove is deep, but does not contact the lingual side. In m3, the posterior lobe is elongated and pointed; the labial groove is deeper, extending very close to the lingual face. In m2 and m3 there is a very small and shallow, centred fossette on the trigonid (that of the m3 has enamel remains). Cement covers the entire tooth in every case.

Vertebrae and girdles. The vertebral column is incomplete. Atlas and axis are missing, but there are 15 cervical and dorsal vertebrae, some of them in anatomical connection (Fig. 4A), and quite complete. The spinous process of the cervical vertebrae is long and narrow, and the transverse process directs forward. Numerous rib fragments are also preserved but are not informative.

The right pelvis and part of the left ilium are preserved united to the sacrum (Fig. 4B). The acetabulum is rather concave and rounded (maximal diameters: 37.4 mm and 41.0 mm). The large obturator foramen is sub-triangular with the following diameters: 64.5 mm × 42.6 mm. There is a sacro–ischiatic fusion, which is unusual among notoungulates, but has already been observed in other mesotheriines (Francis 1965; Shockey *et al.* 2007). There is a bony, rough prolongation that starts at the anteromedial corner of the ischiatic tuberosity, forming a bridge that enlarges as a flattened plate when reaches the sacrum at the transverse process of the penultimate vertebra; consequently, a large dorsal foramen results between sacrum, ilium and ischium.

Long bones. The humerus (Fig. 4C; Table 3) is represented by the rather complete right one and the left distal half. The proximal articulation is rather directed backwards with respect to the distal epiphysis. The proximomedial trochanter is poorly developed, and lacks the anterolateral 'trochanter', from where the deltoid crest projects laterally and then anteriorly ending in a marked tuberosity. At this level, slightly more distally and at the lateral border, the epicondylar crest begins and extends to the distal epiphysis. The distal epiphysis is not very wide, with the lateral epicondyle gently projecting laterally. The medial epicondyle hardly surpasses transversely the medial articular border. The throclea, with a strongly acute medial border, is very concave; it continues laterally in the convex surface of the capitulum, which becomes acute posteriorly. The supra-trochlear foramen is small; this area is badly preserved and the limits of the foramen are not clear. The coronoid fossa is low and wide, without a differentiated radial fossa. The olecranon fossa is deeper, similar in size and shape.

Both radii and ulnae are almost complete. Proximally, the radius rests almost laterally on the ulna, whereas distally it articulates with the medial face of the ulna. The ulna is a robust bone (Fig. 4D). The olecranon, medially curved and lacking its proximal end, would not be very long. The proximal end of the humeral facet projects anterolaterally; it continues distally and medially in a wide, rather flattened surface, which forms a crest with the radius facet. The latter is elongated and low, and laterally oriented. The diaphysis is narrow, but with a great anteroposterior diameter (Table 3), sub-rectangular in cross-section with slight medial and lateral concavities. Distally, it projects posteriorly and on the posterolateral border into small carpal facets.

The radius is a slender bone with enlarged distal epiphysis (Fig. 4E). The humeral facet almost entirely occupies the proximal epiphysis; it is anteriorly pointed, inclined downward. The ulnar facet is fusiform and does not reach the small posterior tuberosity. Distally, there is a small ulnar facet, placed on a distolateral projection, and a great distal sub-triangular, rounded articulation for the scaphoid and the semilunate. The anterolateral face of the distal epiphysis presents two thin crests for ligament insertion.

The two tibiae are represented by a proximal right half and a distal left one (Fig. 5A–B). Proximal facets form a smooth crest between them. The lateral border of the epiphysis is slightly elevated, forming a concavity below. The anterior tuberosity is centred, rounded, from where

Table 3. Dimensions (mm) of the long bones of *Plesiotypotherium casirense* sp. nov., MNHN-Bol-V 003724.

		prox. art.		max. TD	diaphysis		dis. epi.		dis. art.	
Humerus	L	TD	APD	delt crest	TD	APD	TD	APD	TD	APD
Right	195.2	43.7	40.9	57.8	26.0	33.1	72.5	41.9	47.0	40.6
Left	—	—	—	—	24.5	34.9	67.6	(44.5)	51.9	42.2

		olecranon		prox. epi.		diaphysis		dis. epi.	
Ulna	L	TD	APD	TD	H	TD	APD	TD	APD
Right	>232	>21	(41.3)	23.5	49.2	15.4	26.6	25.0	33.6
Left	> 240	> 22	(45.7)	22.9	49.5	15.8	28.0	27.1	29.5

		prox. epi		diaphysis		dis. epi		dis. art	
Radius	L	TD	APD	TD	APD	TD	APD	TD	APD
Right	189.0	35.7	21.2	15.0	14.5	44.9	29.0	32.4	18.6
Left	187.9	34.5	21.5	14.6	14.2	42.5	29.2	31.6	22.0

		prox. epi.		diaphysis		dis. epi.		dis. art.	
Tibia	L	TD	APD	TD	APD	TD	APD	TD	APD
Right	—	60.7	56.3	(16)	(28)	—	—	—	—
Left	—	—	—	15.6	23.8	36.9	30.6	26.3	21.8

		prox. epi.		diaphysis		dis. epi	
Fibula	L	TD	APD	TD	APD	TD	APD
Right	—	32.1	21.3	—	—	—	—
Left	—	—	—	8.9	10.3	18.4	28.5

the tibial crest extends along half diaphysis, with a small tuberosity at the end. The distal fragment shows a triangular cross-section, but rather flattened, enlarging distally. The distal epiphysis, instead, is not very wide. The astragalar facet is quite symmetrical. The medial apophysis projects medially and distally.

A proximally incomplete left fibula (Fig. 5C) shows a very thin diaphysis and an enlarged distal epiphysis (Table 3), with a large facet medially placed. A proximal fragment fits well with the right tibia on its posterolateral area, and presents a large inclined facet over an extended lateral tuberosity.

Carpal and tarsal bones. A right scaphoid presents a very convex anteroproximal facet, laterally displaced, followed posteriorly by a strong tuberosity that does not project distally beyond the distal articulation (Fig. 5D, Table 4). Medially, there is a high anterior facet that projects backwards at its proximal area, oriented posteromedially; another medial facet, high and narrow, is placed posteriorly, over the tuberosity. The anterior face is very narrow at its distal half. Distally, there is a small facet followed by another one very wide and medially elevated (Fig. 5D); it is subdivided by a smooth crest.

The semilunate is wider and shorter than the scaphoid. Its proximal facet is convex and long, narrowing posteriorly (Fig. 5E). There is a projecting lateral tuberosity, at a lower level, that gives a general quadrangulate outline. Medially, there is a wide articulation, high and very concave at its proximal, longer (in APD) half. Another smaller, rounded facet is placed over a posterior tuberosity. Laterally there is a concave, irregular facet. The anterior face is short (Table 4), its upper border convex and the lower one an open V due to the angle between the distal facets. These are similarly developed, the medial one being somewhat wider and shorter, and both convex-concave in APD (Fig. 5E).

Two relatively large bones are recognized as right and left pisiforms (Fig. 5F; Table 4). They are formed by a pear-shaped facet, behind which the bone narrows and projects in a long apophysis. The widest area of the facet is subdivided and very concave, and the rest is smoothly convex.

The trapezoid is a triangular bone (Fig. 5G), slightly wider than long (APD; Table 4). The proximal facet is smaller than the distal one; the former continues medially and laterally into respective facets badly defined.

The magnum is an irregular bone, with an acute border between distal and medial facets (Fig. 5H, I). There is a

Table 4. Dimensions of carpal, tarsal and sesamoid bones of *Plesiotypotherium casirense* sp. nov., MNHN-Bol-V 003724.

Scaphoid	TD ant.	APD max.	H max.	
	19.8	26.5	20.2	
Semilunate	TD ant.	TD max.	H max.	APD max.
	24.6	25.7	18.4	23.9
Pisiform	L max. art.	H max. post.	APD max.	
	22.2	17.4	36.3	
Trapezium?	TD max	TD art.	APD max.	H max.
	9.4	8.3	18.2	17.5
Trapezoid	TD max.	APD max.	H max.	
	18.5	15.8	12.3	
Magnum	TD max	APD max.	H max.	H ant.
	15.0	21.6	13.1	16.9
Unciform	TD max.	APD max.	H max.	
	22.0	17.0	17.0	

		Tuber		Min. post.	Sust. tali	Max. distal		Art. dis.	
Calcaneum	H	TD	APD	TD	TD	TD	APD	TD	APD
	75.6	24.4	24.7	15.7	30.9	22.9	34.0	(19)	26.0

			Throclea		Art. dis.	
Astragalus	TD max.	H max.	TD	H	TD	APD
	39.0	39.7	20.0	33.5	22.2	17.9

Navicular	TD max.	APD max.	H max.
	29.9	30.2	23
Mesocuneiform	TD max.	APD max.	H max.
	13.6	16.6	10.0
Ectocuneiform	TD max.	APD max.	H max.
Right	14.6	28.2	13.9
Left	15.5	28.8	13.6
Sesamoid	TD max.	APD max.	H max.
	14.5	23.0	8.8

large medial facet, anteroproximally projected and very concave, and less concave and higher in the posterior half.

The proximal facet of the unciform continues into the lateroposterior facet, which is in turn subdivided by a smooth crest (Fig. 5H). There is a unique medial articulation corresponding to the magnum and the Mc III; the area for the magnum occupies the whole APD of the medial face (Fig. 5J). In anterior view, the outline of the bone is quadrangular with a laterodistal extension (Table 4).

The calcaneum (Fig. 5K) has the anterolateral facet for the astragalus long and convex-concave as a whole, but relatively flattened; it projects proximally in such way that the astragalus almost contacts the ‘neck’ of the calcaneum in anatomical position. The medial astragalar facet is isolated, although its distal border contacts with the wide, irregular cuboid facet. The sustentaculum is short. The distal APD is greater than the proximal one (Table 4).

The astragalus (Fig. 5L, Table 4) has an asymmetrical trochlea, with an acute lateral lip that is well elevated in comparison with the medial one, which drops smoothly towards a medial tuberosity. The navicular facet is very convex, well separated from the trochlea, and medially displaced. On the posterior face, there are two calcaneum facets; the lateral one is elongated and narrow, very concave proximally, and with its distolateral border projecting laterally. The second facet is separated by a deep groove; it is shorter than the other, but still higher than it is wide, and it contacts distally with the navicular facet.

The navicular has a rounded, concave proximal facet occupying most of the face; two well-developed tuberosities project posterolaterally and posteromedially. The distal face shows the three facets for the cuneiforms (Fig. 5M), separated by crests, the entocuneiform facet being smaller, rounded, and oriented posteromedially. Laterally, there is a facet for the cuboid, which is ovoid, smoothly concave, and

Table 5. Dimensions of metacarpal and metatarsal bones of *Plesiotypotherium casirense* sp. nov., MNHN-Bol-V 003724.

		Prox. epi.		Prox. art.		Diaphysis		Max. dis.	Dis. art.	
	L	TD	APD	TD	APD	TD	APD	TD	TD	APD
Mc I	48.8	13.1	10.1	12.0	10.0	6.5	5.9	7.2	6.3	8.6
Mc II	80.9	20.8	21.1	17.2	19.3	14.3	11.8	19.2	17.8	13.6
	82.4	19.6	21.9	17.4	19.8	14.3	12.2	19.6	17.0	(14)
Mc III	79.8	19.7	22.7	17.7	22.5	12.9	11.7	19.3	16.2	(13.5)
	81.8	20.3	22.8	19.1	22.6	13.8	10.7	19.2	16.4	13.8
Mc IV	73.6	23.3	21.7	19.5	19.9	12.8	11.9	18.4	16.1	13.7
	74.1	23.7	20.2	21.2	19.6	13.7	11.1	17.8	16.5	13.1
Mc V	63.6	11.9	19.5	8.8	18.3	9.9	8.7	14.4	12.9	11.4
Mt I/V?	30.4	6.9	8.0			4.1	4.8		4.7	4.4
	32.3	6.4	6.6			3.6	3.0		4.2	3.9
						4.5	4.1		5.9	7.8
Mt II	62.2	13.5	18.8	11.9	17.3	11.9	9.2	16.3	14.2	10.8
	62.2	13.6	19.4	12.7	18.1	11.6	10.0	16.2	14.4	10.9
Mt III	64.2	16.7	23.2	15.6	20.3	12.5	9.6	18.2	14.8	11.9

higher in its posterior half; its proximal border forms an acute angle with the proximal facet.

The mesocuneiform is a small bone with proximal and distal faces completely occupied by the respective smoothly concave facets (Fig. 5N, Table 4). Medially, there is a subrectangular facet at the posterior part of the face. Laterally, there is a continuous articular surface, but differentiated into an anteroproximal part and a posterior one that occupies the whole height.

The ectocuneiforms are long (in APD) and narrow (Table 4). Proximally there is a kidney-shaped, concave facet, and distally, a similar one, less curved and slightly subdivided in anteroposterior direction (Fig. 5O). There are no medial or lateral facets differentiated.

In addition to the previous described postcranial elements, there exist two others that are tentatively identified. The first is a small bone irregularly outlined, with a concave, ovoid facet and a great apophysis posterior to the facet, flattened on one side and pointing on the other side as well as posteriorly (Fig. 5P, Table 4); it could be the trapezium, though it does not fit with the preserved trapezoid. The other is a small bone with a relatively large facet on one face, and a rough, smoothly convex surface longer than the facet on the opposite side (Fig. 5Q; Table 4). This bone seems to correspond to the sesamoid articulating with the radius described by Shockey *et al.* (2007, fig. 3B), although it evidently has been separated from it; according to these authors this kind of sesamoid is also present in *Trachytherus* Ameghino 1889.

Metacarpals and metatarsals. Most metapodials are preserved, not all complete, and the right Mc I, II and V are missing. The manus is pentadactyl, with Mc I very reduced, but preserving proximal and distal articulations. Mc V is also smaller than Mc II–Mc IV, but clearly more developed than Mc I. In anatomical position, each metapodial overlaps the following one from Mc II to Mc V; the latter does not project laterally beyond the proximal epiphysis of Mc IV (Fig. 6B).

Mc I has a rounded proximal epiphysis, with a smoothly convex facet surrounded by a small tuberosity. The articulation with Mc II is not well defined. Its length is two-thirds that of Mc II (Table 5). The diaphysis narrows distally and does not enlarge at the distal epiphysis, which bears a well-developed trochlea. Only the left Mc I was preserved.

Mc II, as well as Mc III and Mc IV, is a relatively robust bone, with distal epiphysis slightly enlarged and diaphysis relatively wide (Table 5). The proximal epiphysis of Mc II is sub-triangular (Fig. 6A). Transversely, its proximal facet is smoothly concave and anteroposteriorly convex-concave. The lateral border forms a strong angle with the anterolateral facet, whereas it passes smoothly to the lateroposterior facet, later forming a sharp crest. Both lateral facets are subdivided. Medially, there are two separated facets, apparently too developed for Mc I. In anterior view, there is a proximolateral tuberosity.

The Mc III has a trapezoidal, irregular proximal facet (Fig. 6A) with a medial notch that separates both medial facets. The proximal articulation is medially inclined, smoothly convex anteroposteriorly. Medial facets are small and convex. The lateral facets are wider, high and narrow. The anterior one has a distal sub-facet that is very concave; the posterior one is smoothly concave.

In anterior view, the Mc IV shows the proximal epiphysis projected laterally (Fig. 6B). The proximal facet is wide, trapezoidal and smoothly convex in both diameters. Medial facets project medially, enlarging the transversal diameter of the epiphysis; they are small, the anterior one very convex and the posterior one more flattened, separated by a deep depression.

The Mc V reaches the length of Mc IV above the distal trochlea (Fig. 6B). Diaphysis and distal epiphysis are similar to the precedent metapodials, but narrower (Table 5). The proximal epiphysis is strongly inclined medially and anteriorly, with the facet occupying all of the face, with a strong medial notch. A small tuberosity extends posterolaterally.

Among the metatarsals, left Mt II and III and right Mt II are complete (Fig. 6C–D). Besides these, there are two complete but very reduced and thin metapodials (thinner than Mc I), with differently developed proximal epiphysis, and a distal fragment of another one, with more developed distal trochlea (Table 5). We are not sure about their identification, and they could be reduced Mt I or Mt V (Fig. 6E).

The Mt II overlaps the Mt III in anatomical position, hardly articulating anteromedially, because the facet mainly corresponds to the tarsal bone; posteriorly there is a better-developed medial facet. Laterally, there is a very small facet placed anteriorly and by the proximal border, which would articulate with a reduced Mt I. In anterior view, there is a pronounced proximal crest, medially placed (Fig. 6C).

Mt III has the proximal facet with lateral and medial notches; it is inclined laterally, smoothly convex anteroposteriorly. The posterior tuberosity is slightly projected over the facet. Medially, the anterior facet is large, oval-shaped, and very concave; the posterior facet, separated by a narrow groove, is rounded and rather smaller than the former (Fig. 6D). The Mt II and Mt III (Table 5) are shorter than Mc II and III.

The other three distal fragments correspond to the left Mt II and right and left Mt IVs.

Phalanges. First, second and third phalanges are well represented, showing differences in length and robustness (Fig. 6F). The third phalanx has a deep dorsal cleft that is shallower distally. There are two narrower third phalanges each without a cleft, likely belonging to the reduced metapodials.

Remarks. As commented above, the mesotheres from Bolivia were mainly studied by Villarroel (1974a, b, 1978) whose research noted the geographical extension of this group of notoungulates outside of Argentina, where they were better known at that time. Villarroel (1974a) described the mesotheriines from Achiri as the genus *Plesiotypotherium* and recognized two species, *P. achirense* and *P. majus*, the latter of greater size. The Achiri specimens correspond to the Late Miocene (younger than 8 Ma). Later, this author added a third species, *P. minus* Villarroel, 1978, from the early Middle Miocene locality of Cerdas (Villarroel 1978). *Plesiotypotherium* was also recognized by Oiso (1991) at the Middle Miocene locality of Nazareno, and Croft (2007) assigned to *P. minus* a pair of mandibles found at Río Rosario (Quebrada Honda fauna, Santacrucian Age). This species has been recently revised by Townsend & Croft (2010), who recognize it as a possible different genus. As already noted, an isolated skull (GB-KKL 740, Fig. 7A) from Casira was succinctly described by Anaya *et al.* (1989), and considered as *Plesiotypotherium* sp. by Croft (2007). In turn, the studied specimen (MNHN-Bol-V-003724), labelled as cf. *P. majus*, was referred to as *Plesiotypotherium* sp. by Shockey *et al.* (2007). Flynn *et al.* (2005) noted a dubious age for the genus *Plesiotypotherium*, from Middle to Late Miocene (?Friasian to ?Chasicoan mammal ages). On the other hand, Villarroel (1974b) described another Bolivian mesotheriine from the Late Miocene of Choquecota, *Microtypotherium choquecotense* Villarroel, 1974b, mainly characterized by its small size. The author correlated this locality with the Friasian fauna from Argentina. Finally, Flynn *et al.* (2005) consider the Friasian or Colloncuran (Middle Miocene) as possible age for *Microtypotherium* Villarroel, 1974b.

A comparison of both skulls from Casira (MNHN-Bol-V-003724, Fig. 2, and GB-KKL 740, Fig. 7A) shows that they present a similar size, the zygomatic arch in each is high and contacts the postorbital apophysis; although the nasals are missing in GB-KKL 740, the posterior border seems to be similar, not markedly W-shaped (Fig. 7A). Anaya *et al.* (1989) indicated that the skull is more robust than that of *P. achirense* (Villarroel 1974a), and with a greater thickness of the sagittal crest, a character that we cannot verify in MNHN-Bol-V-003724. The skull GB-KKL 740 is presently stored at the MNHN in La Paz, but it had been broken into two fragments, and has lost several parts as the zygomatic arches and the anterior extremity of the rostrum. The parastyle of M2–M3 in MNHN-Bol-V-003724 is more detached than in GB-KKL 740 (at the breakage level of the molars). The general similarity of GB-KKL 740 to MNHN-Bol-V-003724 leads us to refer it to the new species, supporting the differences with respect to *P. achirense* stated by Anaya *et al.* (1989).

Compared with the skull GB-ACH 228 (Fig. 7B–D) labelled as *Plesiotypotherium achirense*, stored in the MNHN, the Casira skull MNHN-Bol-V-003724 (Fig. 2) presents several differences. The zygomatic arch has its inferior border straighter or slightly concave, and it forms two marked posterodistal and anterodistal angles, contrary to the more continuous convexity of GB-ACH 228, which is similar to the condition in the holotype (ACH 26) of *P. achirense* (Villarroel 1974a). The posterior part of the arch is very wide (in APD) in the three specimens. The nasals seem to be proportionally less enlarged posteriorly in MNHN-Bol-V- 003724, and the posterior border is not so markedly W-shaped as in GB-ACH 228 (maximum/minimum – in the fragment – width: 58.9/28.1 mm); the paratype of *P. achirense* (Villarroel 1974a, pl. II) preserves both complete nasals, and they seem to be proportionally longer and narrower (dimensions are not provided by the author) than the holotype and MNHN-Bol-V- 003724. The lacrimal bone is not very well preserved, but it presents one foramen together with a bony process similar to GB-ACH 228 and the holotype. In ventral view, the zygomatic plate starts at the level of P4 and its posterior border is concave, reaching the level of the anterior part of M3, whereas in GB-ACH 228 (Fig. 7C) it starts at the level of the third lobe of M1, and its posterior border is slightly concave (posterior end of M3 level), as happens in the holotype. In the same view, the glenoid articulation forms a smoothly concave posterior profile in MNHN-Bol-V-003724, which is straight in the other specimen. General dimensions (Table 1) are somewhat greater in the studied specimen than in *P. achirense* (Villarroel 1974a); for instance, total length surpasses 248 mm × 218 mm of the holotype; estimated bizygomatic width is around 168 mm, and is 134.8 mm in *P. achirense*; palatal length/width is 138.4/68 mm × 120/49.8 mm.

The holotype (ACH 27) of *P. majus* (Villarroel 1974a, pl. 2) shows a relatively shorter zygomatic plate, starting at the level of the first lobe of M1 and reaching the second lobe of M3; its posterior border is concave similarly to the Casira specimen. The postpalatine apophyses of *P. majus* form a wider angle between them and are less elongated than in MNHN-Bol-V-003724. Dimensions of our specimen are also greater than those of *P. majus* (e.g. bizygomatic width, 142 mm; palatal width, 53.8 mm), a species defined as larger and more robust than *P. achirense* (Villarroel 1974a, p. 277).

The mandible presents a similar aspect to that of *P. achirense* (Villarroel 1974a), with greater dimensions (Table 1) and a wider mandibular incision between the coronoid process and the mandibular condyle; the posterior border is clearly more convex in the studied specimen.

Dental morphology differs in several features. P3 and P4 do not have a lingual fold either in MNHN-Bol-V-003724 or *P. achirense* and *P. majus*, but our specimen presents a narrower and more projected parastyle, with more marked groove, and more convex paracone fold in P4. In addition, the M3 presents a simple third lobe (Fig. 3A), whereas the holotype of *P. achirense* has a neat posterolingual groove that subdivides the lingual portion of that lobe, which results in a more lingually elongated M3. This fold does not appear in M1–M2 but a smooth undulation (M2) or a very tiny fold (M1) is present in the same area (GB-ACH 228; Fig. 7C and holotype of *P. achirense*). This fold is neither present in the specimen considered with doubts as *P. achirense* by Villarroel (1974a, fig. 9A; the specimen number is not detailed). In contrast, the Casira specimen presents a small but marked posterolingual groove in M1, but none in M2–M3; the groove in M1 is more posteriorly placed than in the M3 of *P. achirense*. In *P. majus*, the M3 presents a rather smoother posterolingual groove; M1 and M2 have none. Tooth size of MNHN-Bol-V-003724 is similar to *P. achirense*, with M3 slightly longer (Table 2), but as for other cranial dimensions, the upper series length (76.4 mm) is greater; it is 69.5 mm in the holotype of *P. achirense*, and 61/62 mm in GB-ACH 228. Dental measurements of *P. majus* are somewhat greater, and the I1 is relatively more labiolingually flattened than in the Casira specimen (Table 2).

As commented in the introduction, another specimen from Achiri (GB-ACH 100), labelled *Plesiotypotherium* sp., was revised at the MNHN-Bol, but it is characterized by a clearly bilobed P4 (EC, pers. obs.) that differentiates it from *Plesiotypotherium*, and makes it similar to other genera such as *Pseudotypotherium* Ameghino, 1904, *Caraguatypotherium* Flynn *et al.*, 2005, or *Mesotherium* Serrés, 1867.

Lower teeth are quite similar in morphology to the holotype of *P. achirense*. After the scheme published by Villarroel (1974a, fig. 10), it seems that the anterior lobe of p4 and the posterior one of m3 are proportionally more elongated than in MNHN Bol-V-003724, but this is not so evident on the photograph of the holotype (Villarroel 1974a, pl. I). The i1/i2 ratio is 1.7 and 1.6 for MNHN Bol-V-003724, 1.5 for *P. achirense*, and 1.4 for the lower incisors assigned to *P. majus*. These values correspond to the condition also observed in *Eutypotherium lehmannistchei* Roth, 1902 following Cerdeño & Montalvo (2001, character state 22^1); however, after Flynn *et al.* (2005), who considered a different coding of this character, *P. majus* corresponds to character state 22^0 and the others to state 1. It is worth noting that the magnitude of difference between states considered by these authors for character 22 is that observed between right and left incisors of our specimen, and also among the three specimens compared; besides, the interval of states 1 and 2 are not equivalent. On the other hand, they codify *P. achirense* as character state 22^0 (as well as *E. lehmannistchei*), whereas for us, it would be 22^1 (after dimensions by Villarroel 1974a).

Concerning the postcranial skeleton, the studied humerus has a deltoid crest (Fig. 4C) more laterally expanded than that of *P. achirense*. After the figure of Villarroel (1974a, fig.12), the humerus of *P. achirense* appears more slender, but this contrasts with the dimensions provided by the author for the total length (93.5 mm), which is less than half that of our specimen (Table 3), whereas the diameters of epiphyses are not so different. This is evidently a typing error, and the value likely was 193.5 mm (agreeing with the figure), which renders a gracility index (TD diaphysis/length) of 0.09, lesser than that of MNHN Bol-V-003724, 0.13. Villarroel also described a large supratrochlear foramen, which contrasts with the small one present in MNHN BOL-V-003724. The radius described by Villarroel (1974a) is also shorter (about 20 mm) than ours. The tibial fragments from Casira are similar to the same bone of *P. achirense*, but the lateral concavity figured by Villarroel (1974a, fig. 15) is more accentuated. The compared dimensions are slightly larger on the Casira specimen. The fibula is not described for *P. achirense*.

Carpal bones are not fully described for *P. achirense*, and dimensions and figures are not provided either (Villarroel 1974a). For the scaphoid, just a concave facet is established for the articulation with the semilunate, but the scaphoid from Casira presents two well-defined medial facets (see description). Concerning tarsus, astragalus, calcaneum and navicular do not present special differences, the size being somewhat greater for the Casira specimen. The calcaneum and the astragalus assigned to *P. majus* (Villarroel 1974a) are greater than those of *P. achirense*, and close to those from Casira, the latter still with some greater dimensions. An astragalus from Achiri stored at the MNHN in La Paz, GB-ACH 233, labelled as ?*Plesiotypotherium*, is very different from the Casira specimen; it is a shorter bone, without detaching distal articulation, which is flattened and expanded posteriorly, and a shorter and wider medial calcaneum facet. This is a rhinoceros-like morphology that can be assigned to a toxodontid, group of notoungulates represented by two species at Achiri (St-André 1993, 1994).

With respect to the sacroischial fusion observed in the Casira specimen (Fig. 4B), Shockey *et al.* (2007, p. 237) noted that the sacroischial reinforcement has already been described for the genus *Mesotherium*, and that this condition, as well as the supernumerary fused vertebrae in the sacral region, is present in a variety of mammals with fossorial habits. They concluded that the appendicular skeleton of three genera of mesotheriids "compare favorably to the hypothetical ideal for a scratch-digging mammal."

Compared with the Late Miocene Argentinean mesotheres, the Casira specimen is closer to the genus *Typotheriopsis* Cabrera & Kraglievich, 1931 than to *Pseudotypotherium* because of the absence of a lingual groove in P4 and the more triangular-outlined upper premolars. *Typotheriopsis chasicoensis* Cabrera & Kraglievich, 1931 (MLP 12–1666; E.C. pers. data) presents less undulating ectoloph in upper molars and marked parastyle in P4, but not so labially projected as in the Casira specimen. The mandible of *T. chasicoensis* has a more marked symphyseal angle. Tooth dimensions of *T. chasicoensis* are very similar to those of MNHN BOL-V-003724, but slightly narrower, and its m3 is relatively longer. The index i1/i2 in *T. chasicoensis* is 2. The greater tooth width is also observed with respect to the lower molars, especially m2–m3, of the specimens from La Pampa Province (Cerdeño & Montalvo 2001), e.g. GHUNLPam 19062. The position of the lingual groove of I1 is similar to that of GHUNLPam 196, 327, and 5998, among others, slightly displaced to the anterior side. However, most material from La Pampa could not be assigned to one or the other genus, due to the lack of diagnostic characters.

More general similarities are observed between MNHN BOL-V-003724 and *Typotheriopsis silveyrai* Cabrera, 1937 from Tupungato, Mendoza Province (Cabrera 1937; E.C. pers. data). Its skull (MLP 36-XI-10 – 2) is rather complete, though not so well preserved and somewhat distorted dorsoventrally. In dorsal view, this skull shows that the frontal narrowing is not as marked as in the Casira specimen, and the lateral borders of nasals seem to be straighter. The profile of the zygomatic arch also presents a marked anterodistal angle. In ventral view, the extension of the zygomatic plate in *T. silveyrai* is shorter and with a less concave posterior border; the premaxillary–maxillary suture is closer to the incisors; and the postpalatal apophyses are much shorter and massive. Upper teeth have more flattened ectoloph, and the P4 is shorter, without such a projected parastyle. Dimensions are slightly larger for the Casira skull.

Flynn *et al.* (2005) described another mesothere from northernmost Chile, *Caraguatypotherium munozi* Flynn *et al.*, 2005, of Middle or Late Miocene age (10–15 Ma), likely constrained to 10.8–11.7 Ma (?Mayoan–Chasicoan age). Following the description and dimensions provided by these authors, *C. munozi* is smaller than the Casira specimen. The nasals appear to be relatively longer and narrow. The zygomatic arch is incomplete, but it seems to have also a marked anterodistal angle. The nasal opening is higher, more widely open. The mandible has a less convex posterior border and the symphyseal angle is more marked.

As a result of this morphological and metric comparison, the Casira specimen is close to the known *Plesiotypotherium* species, but it presents differences that allow a specific separation. A cladistic analysis is performed to check the phylogenetic relationships of this material.

Phylogenetic analysis

The phylogenetic relationships of mesotheres have been previously inferred by means of cladistic analyses by Cerdeño & Montalvo (2001), Croft *et al.* (2004) and Flynn *et al.* (2005). Reguero & Castro (2004) also performed a cladistic analysis of the group in order to place the new proposed trachytheriine taxon (*Anatrachytherus soriai* Reguero & Castro, 2004), and therefore including the Trachytheriinae species as terminal taxa. More recently, Billet *et al.* (2008) considered this species as synonymous with *Trachytherus spegazzinianus* Ameghino 1889 and presented a phylogenetic analysis focused on the Trachytheriinae, including only two Mesotheriinae genera. The matrix presented by Croft *et al.* (2004) is the most complete, because it includes the mesotheriines from the Chucal Formation (Chile) and adds one more character (No. 29) to the list presented by Flynn *et al.* (2005).

In the present attempt we composed a data matrix of 22 taxa and 39 — 15 cranial and 24 dental characters (Appendices 1–2; see Online Supplementary Material), with the same outgroups: Family Archaeohyracidae and Subfamily Trachytheriinae, the closest groups to mesotheriines. Following Cerdeño & Montalvo (2001), only two species are considered for Argentina during Late Miocene period (Huayquerian Age): *Typotheriopsis silveyrai* and *Pseudotypotherium subinsigne* (Rovereto, 1914). A comment

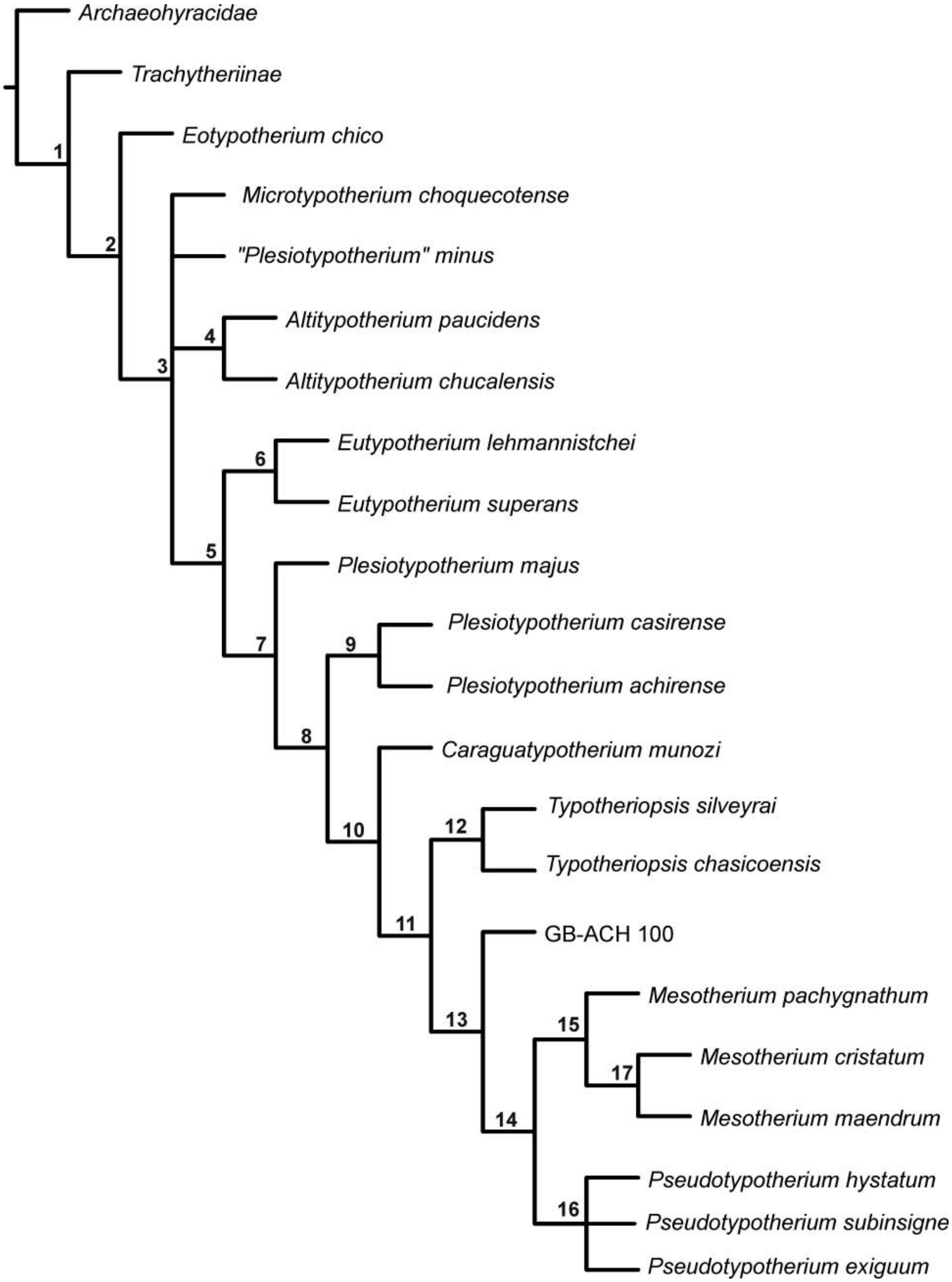

Figure 8. Consensus tree of the cladistic analysis of Mesotheriinae. Numbers refer to nodes. Note synapomorphies as follows: Node 2: 7^2, 26^1, 35^1; Node 3: 9^2, 23^1, 24^1; Node 4: 19^4, 22^1; Node 5: 19^2, 28^1, 34^2; Node 6: 7^0; Node 7: 3^2; Node 8: 33^1; Node 9: 6^0, 11^1; Node 10: 16^1, 31^2; Node 11: 2^2; Node 12: 22^1; Node 13: 24^3, 34^3; Node 14: 16^2, 25^1, 26^2, 31^3, 37^1; Node 15: 5^0, 18^2, 27^2; Node 16: 4^1; Node 17: 1^2, 3^3, 6^2.

is needed on the generic status of *P. hystatum* Cabrera, 1937, a species described within *Pseudotypotherium*, which appears in the previous analyses by Croft *et al.* (2004) and Flynn *et al.* (2005) as *Mesotherium hystatum* (or *M. hystatum*) in text, table and figures. Due to the position of this species in their cladograms (closer to *Pseudotypotherium* species than to other *Mesotherium* species) and the absence of any comment on this matter, we think this is just an error that could come from table 5 in Cerdeño & Montalvo (2001), where it mistakenly appears as *M. hystatum* (not in text and cladogram).

The data matrix (Appendix 2 in Online Supplementary Material) was analysed using Maximum Parsimony under equal and implied weights with the computer program TNT 1.1 (Goloboff *et al.* 2008), and characters were treated as unordered. We conducted heuristic searches with TBR (Tree Bisection Reconnection) and explored a wide range of concavity values ($K = 1–100$) during the implied weights searches. With respect to the matrix in Croft *et al.* (2004), we have modified the character referred to the postorbital apophyses (No. 4 in our list, Appendix 1 in Online Supplementary Material), due to the observation of transversely placed apophyses that are either in contact or not with the zygomatic arch. We also added a fourth state to the character concerning the root of the zygomatic arch (No. 7 in our list), regarding the beginning of the arch at the level of P4. Also, we adapted character 6 in Flynn *et al.* (2005) into two separate characters (Nos. 5 and 6 in our list). Furthermore, we added new characters that refer to: anterodistal angle of the zygomatic arch (No. 8); the concavity of the posterior border of the zygomatic plate (No. 10); the presence of a bony process on the lacrimal foramen (No. 11); the presence of a posterolingual groove in the third lobe of M1 (No. 30), and the presence of a posterolingual groove in the third lobe of M3 (No. 32).

The analysis under implied weights (where $K > 9$ topologies are stable) resulted in three most parsimonious topologies of 108 steps with a consistency index (CI) of 0.69 and a retention index (RI) of 0.75. The strict consensus tree (Fig. 8) indicates that the monophyly of the subfamily Mesotheriinae is supported by three synapomorphies (node 2: 7^2, 26^1, 35^1). This node places *Eotypotherium chico* Croft *et al.*, 2004 as sister group of the other terminal taxa. The following node 3 is a major polytomy composed of *Microtypotherium choquecotense*, '*Plesiotypotherium*' *minus*, the clade formed by the species of *Altitypotherium* Croft *et al.*, 2003 (node 4: 19^4, 22^1), and the remaining taxa gathered in node 5 (19^2, 28^1, 34^2). Within the latter, several genera are supported as monophyletic clades: *Eutypotherium* Roth, 1902 (node 6: 7^0), *Typotheriopsis* (node 12: 22^1), *Mesotherium* (node 15: 5^0, 18^2, 27^2), and *Pseudotypotherium* (node 16: 4^1), though the relationships among the three species of the latter are not resolved. Instead, *Plesiotypotherium* appears to be paraphyletic, with *P. majus* as sister group of the clade composed of *P. casirense* and *P. achirense* (node 9: 6^0 and 11^1) plus the remaining taxa (node 10). *P. majus* presents only one character differently coded from *P. achirense*, but 13 characters remain as missing data. *P. casirense* presents two autapomorphies (8^1 and 10^1). The synapomorphies of *P. casirense* and *P. achirense* (6^0 and 11^1) refer to a large infraorbital foramen and a lacrimal foramen with bony process, the former appearing as a parallelism with *Pseudotypotherium*, whereas the latter is an autapomorphy of *Plesiotypotherium* (the condition of both features in *P. majus* is unknown). The generic diagnostic characters established by Villarroel (1974a; dental imbrication similar to that of Trachytheriinae; length i1/i2 ratio about 1.5; parallel or slightly, anteriorly divergent diastemas; large infraorbital foramen and deep suborbital fossa) do not appear as synapomorphies of the genus in the cladistic analysis.

Our current analysis did not result in many differences from previous analyses (Cerdeño & Montalvo 2001; Flynn *et al.* 2005; Shockey *et al.* 2007). One difference is the position of *Caraguatypotherium munozi*, which appears in our analysis as the sister group (node 10) of the clade formed by *Typotheriopsis*, GB-ACH 100, *Mesotherium* and *Pseudotypotherium*. The specimen GB-ACH 100 does not appear to be related to *Plesiotypotherium*, supporting our interpretation of its morphological features (see Remarks). The analysis places it closer to the *Pseudotypotherium* and *Mesotherium* clades, sharing two unambiguous synapomorphies (node 13: 24^3 and 34^3).

Conclusions

The detailed study of the mesotheriine skeleton MNHN-Bol-V-003724 from the Late Miocene Casira locality, southern Bolivia, indicates that the specimen should be identified as a new species of the genus *Plesiotypotherium*, *P. casirense* sp. nov. It displays some general similarities with the species *P. achirense*, but bears particular cranial and dental characteristics, as well as larger and more robust postcranial bones. A number of postcranial elements are described in detail for the first time for *Plesiotypotherium*. The assignment to this genus is supported by the phylogenetic analysis, where both species constitute a monophyletic clade. *P. majus*, however, is not included in this clade and, consequently, the genus appears paraphyletic. The partial skull GB-KKL 740 from Casira, previously described by Anaya *et al.* (1989) is also referred to the new species, supporting the interpretation of these authors about its differences with respect to *P. achirense*.

The specimen GB-ACH 100 from the Bolivian locality of Achiri is considered to be different to *P. achirense* from the same site, and this is reflected in the phylogenetic analysis; it is closer to the genera *Pseudotypotherium* and *Mesotherium*.

The new taxon increases the known diversity of the Family Mesotheriidae in the Miocene of Bolivia and the South American faunal context.

Supplementary material

Supplementary material can be viewed online: DOI: 10.1080/14772019.2011.569576

Acknowledgements

We thank the reviewers and the editor of the journal for the critical review of the manuscript and their valuable comments. Special thanks are due to the Director and the staff of the Museo Nacional de Historia Natural in La Paz (Bolivia) for facilitating the study of the palaeontological collection. S. Roig and B. Ferrero helped with the phylogenetic analysis. This research was partially financed by the Institut pour la Recherche et le Développement (IRD, France) in Bolivia, the Cultural Service of the French Embassy in Bolivia, and the Consejo Nacional de Investigaciones Científicas y Técnicas (CONICET) of Argentina.

References

Alston, E. R. 1876. On the classification of the Order Glires. *Proceedings of the Zoological Society of London*, **1876**, 61–98.

Ameghino, F. 1889. Contribución al conocimiento de los mamíferos fósiles de la República Argentina. *Actas de la Academia Nacional de Ciencias de Córdoba, Buenos Aires*, **6**, 1–1027.

Ameghino, F. 1904. Nuevas especies de mamíferos cretáceos y terciarios de la República Argentina. *Anales de la Sociedad Científica Argentina de Buenos Aires*, **57**, 162–175.

Anaya, F., **Pachero, J.** & **Pili, L. A.** 1989. Hallazgo de mesotherinos en la formación Kasira (Terciario) en el Sud Boliviano, Prov. Modesto Omiste-Dpto. Potosí. *Boletín del Servicio Geológico de Bolivia, La Paz, Serie A*, **4**, 41–46.

Billet, G., **de Muizon, C. de** & **Mamaní Quispe, B.** 2008. Late Oligocene mesotheriids (Mammalia, Notoungulata) from Salla and Lacayani (Bolivia): implications for basal mesotheriid phylogeny and distribution. *Zoological Journal of the Linnean Society*, **152**, 153–200.

Cabrera, A. 1937. Notas sobre el suborden Typotheria. *Notas del Museo de La Plata, Paleontología*, **2**(8), 17–43.

Cabrera, A. & **Kraglievich, L.** 1931. Diagnosis previas de los ungulados fósiles del Arroyo Chasicó. *Notas Preliminares del Museo de La Plata*, **1**, 107–113.

Cerdeño, E. & **Montalvo, C.** 2001. Los Mesotheriinae (Mesotheriidae, Notoungulata) del Mioceno Superior de La Pampa, Argentina. *Revista Española de Paleontología*, **16**, 63–75.

Croft, D. A. 2007. The Middle Miocene (Laventan) Quebrada Honda Fauna, Southern Bolivia and a description of its Notoungulates. *Palaeontology*, **50**, 277–303.

Croft, D. A., **Flynn, J. J.** & **Wyss, A.R.** 2004. Notoungulata and Litopterna of the early Miocene Chucal Fauna, Northern Chile. *Fieldiana: Geology*, **50**, 1–52.

Flynn, J. J., **Croft, D. A.**, **Charrier, R.**, **Wyss, A.R.**, **Hérail, G.** & **García, M.** 2005. New Mesotheriidae (Mammalia, Notoungulata, Typotheria), geochronology and tectonics of the Caragua area, northernmost Chile. *Journal of South American Earth Sciences*, **19**, 55–74.

Francis, J. C. 1965. Los géneros de la subfamilia Mesotheriinae (Typotheria, Notoungulata) de la República Argentina. *Boletín del Laboratorio de Paleontología de Vertebrados*, **1**, 7–23.

Goloboff, P., **Farris, J.** & **Nixon, K.** 2008. TNT, a free program for phylogenetic analysis. *Cladistics*, **24**, 774–786.

Oiso, Y. 1991. New land mammal locality of middle Miocene (Colloncuran) age from Nazareno, southern Bolivia. Pp. 653–672 in R. Suárez-Soruco (ed.) *Fósiles y Facies de Bolivia – Vol. I Vertebrados*. Yacimientos Petrolíferos Fiscales Bolivianos: Santa Cruz.

Reguero, M. & **Castro, P.** 2004. Un Nuevo Trachytheriinae (Mammalia, †Notoungulata) del Deseadense (Oligoceno tardío) de Patagonia, Argentina: implicancias en la filogenia, biogeografía y bioestratigrafía de los Mesotheriidae. *Revista Geológica de Chile*, **31**, 45–64.

Roth, S. 1902. Notas sobre algunos nuevos mamíferos fósiles. *Revista del Museo de La Plata*, **10**, 251–256.

Roth, S. 1903. Los ungulados sudamericanos. *Anales Museo de La Plata, Paleontología*, **5**, 5–36.

Rovereto, C. 1914. Los estratos araucanos y sus fósiles. *Anales del Museo Nacional de Historia Natural, Buenos Aires*, **25**, 1–249.

Serrés, M. 1867. De l'ostéographie du *Mesotherium* et de ses affinitiés zoologiques. *Comptes Rendus des Séances de l'Académie de Sciences de Paris*, **65**(2), 6–17, 140–148, 273–278, 429–437, 593–599, 740–748, 841–848.

Shockey, B. J., **Croft, D.** & **Anaya, F.** 2007. Analysis of function in the absence of extant functional homologues: a case study using mesotheriid notoungulates (Mammalia). *Paleobiology*, **33**, 227–247.

St-André, P.-A. 1993. *Hoffstetterius imperator* n. g., n. sp. du Miocène supérieur de l'altiplano bolivien et le statut des Dinotoxodontinés (Mammalia, Notoungulata). *Comptes Rendus de l'Académie des Sciences de Paris*, **316**, 539–545.

St-André, P.-A. 1994. *Contribution à l'étude des grands mammifères du Néogène de l'altiplano bolivien*. Unpublished PhD Thesis, Muséum National d'Histoire Naturelle, Paris, 564 pp.

Townsend, K. E. B. & **Croft, D.** 2010. Middle Miocene mesotheriine diversity at Cerdas, Bolivia and a reconsideration of *Plesiotypotherium minus*. *Palaeontologia Electronica*, **13**(1), 36 pp.

Villarroel, C. 1974a. Les Mésothérinés (Notoungulata, Mammalia) du Pliocène de Bolivie. Leurs rapports avec ceux d'Argentine. *Annales de Paléontologie*, **60**, 245–281.

Villarroel, C. 1974b. Un Mésothériiné nouveau (Notoungulata, Mammalia) dans le Miocène supérieur de Bolivie. *Comptes Rendus de l'Académie des Sciences de Paris*, **279**, 551–554.

Villarroel, C. 1978. Edades y correlaciones de algunas unidades litoestratigráficas del Altiplano boliviano y estudio de algunos representantes mesotheriinos. *Revista de la Academia Nacional de Ciencias de Bolivia*, **1**, 159–170.